Available online at www.sciencedirect.com

SCIENCE DIRECT®

Journal of Computational and Applied Mathematics 168 (2004) 155–164

JOURNAL OF COMPUTATIONAL AND APPLIED MATHEMATICS

www.elsevier.com/locate/cam

Fatigue crack growth analysis by an enriched meshless method

Marc Duflot*,[1], Hung Nguyen-Dang

Fracture Mechanics Group, University of Liège, Chemin des chevreuils 1, Liège 4000, Belgium

Received 26 September 2002; received in revised form 17 April 2003

Abstract

The aim of this paper is to analyze the fatigue growth of cracks under cyclic loading conditions. The propagation is modeled by successive linear extensions, which are determined by the stress intensity factors (SIFs) obtained after a linear elastic analysis. We use a meshless method to perform the successive analyses. A new contribution of this paper is that we add to the fixed set of nodes three nodes with a special weight function at each crack tip. This is done in order to accurately catch the stress singularity at these tips. We verify on simple problems that the enriched method gives more accurate SIFs than the classic method. Then, we apply it to a fatigue crack growth problem.

Keywords: Fatigue; Crack propagation; Meshless method

1. Introduction

The aim of this paper is to analyze the fatigue growth of cracks under cyclic loading conditions. The propagation is modeled by successive linear extensions, which are determined by the stress intensity factors (SIFs) obtained after a linear elastic analysis. More precisely, we use a generalized Paris' law to compute the propagation direction and the increment length at each crack tip, knowing both modes I and II SIFs.

The classic finite element method is not appropriate to perform the successive analyses because it is expensive to remesh the domain after each crack extension. We use a meshless method, which proved in a number of papers to be efficient for fracture mechanics problems, see for example [3].

* Corresponding author.
E-mail address: m.duflot@ulg.ac.be (M. Duflot).
[1] Supported by the Belgian National Fund for Scientific Research (F.N.R.S.).

0377-0427/$ - see front matter
doi:10.1016/j.cam.2003.04.006

A new contribution of this paper is that we add to the fixed set of nodes three nodes at each crack tip. This is done in order to accurately catch the stress singularity at these tips. These nodes have special weight functions and they move with the tips. The weight functions of these special nodes possess the behavior in $\sqrt{r}$ near the tip and exhibit an angular variation similar to the exact near-tip displacement field. They have a local support like the regular weight functions. This enrichment can easily and naturally be implemented in an existing meshless method program. Moreover, the computational cost of this enriched method is nearly the same as the classic method.

We first verify on two simple problems that the enriched method gives more accurate SIFs than the classic method. We then apply it to a fatigue crack growth problem, consisiting of two crack tips propagating towards each other and stopping when the two cracks overlap. We compare the fatigue life diagram and the crack paths predicted by this method to results obtained by a boundary element method [9]. Good agreement is observed. This last presented example shows that our method is able to model quite complicated extensions.

2. Meshless method

First, we briefly recall the basis of the meshless method for the resolution of partial differential equations (PDEs). It consists in using the shape functions (2), built without having recourse to a mesh, as the test functions and the trial functions in the variational principle of the PDEs. In this paper, the PDEs under consideration are the equilibrium equations of two-dimensional, homogeneous, isotropic and linear-elastic solids undergoing small displacements. We only mention the equations that we need in the following and refer to the overview paper [2] for all the details.

Consider a set of N nodes scattered in a domain Ω and let $\mathbf{x}_i$ be the coordinates of node i. The moving least-squares approximation $\mathbf{u}^h(\mathbf{x})$ of a (multi-dimensional) field $\mathbf{u}(\mathbf{x})$ in Ω is

$$\mathbf{u}^h(\mathbf{x}) = \sum_{i=1}^{N} \phi_i(\mathbf{x})\mathbf{u}_i, \tag{1}$$

where $\mathbf{u}_i$ is the value of the field $\mathbf{u}$ at $\mathbf{x}_i$ and ϕ_i is the shape function of node i, given by

$$\phi_i(\mathbf{x}) = \mathbf{c}^{\mathrm{T}}(\mathbf{x})\mathbf{p}(\mathbf{x}_i)w_i(\mathbf{x}), \tag{2}$$

where $\mathbf{p}(\mathbf{x})$ is a set of basis functions, $w_i(\mathbf{x})$ is a weight function associated with the node i and

$$\mathbf{c}(\mathbf{x}) = \mathbf{A}^{-1}(\mathbf{x})\mathbf{p}(\mathbf{x}) \tag{3}$$

with

$$\mathbf{A}(\mathbf{x}) = \sum_{i=1}^{N} w_i(\mathbf{x})\mathbf{p}(\mathbf{x}_i)\mathbf{p}^{\mathrm{T}}(\mathbf{x}_i). \tag{4}$$

In practice, the weight functions are positive in order to provide a positive definite $\mathbf{A}$ matrix which ensures that the approximation is well-behaved. Moreover, a small domain Ω_i containing $\mathbf{x}_i$ is associated with node i such that $w_i(\mathbf{x})$, and as a result $\phi_i(\mathbf{x})$, equal zero outside Ω_i. This choice is made in order to provide the approximation with a local character and to restrict the sums in Eqs. (1) and(4) to a few terms. Finally, the common choice in the literature is that $w_i(\mathbf{x})$ decreases with the

distance between $\mathbf{x}_i$ and $\mathbf{x}$, in such a way that the nearer a node is to a point, the more it influences this point. This choice is revised in Section 3.

In the following, we always use a linear basis: $\mathbf{p}^{\mathrm{T}} = [1, x, y]$, which proved to be a good trade-off between speed and efficiency. The enriched method that is described hereafter however also works with other basis. We decide to use the same weight for each regular node (in contrast with the enriched nodes): a quartic weight function on a circular support

$$w_i(\mathbf{x}) = S_4(s), \tag{5}$$

where we use the quartic spline

$$S_4(s) = \begin{cases} 1 - 6s^2 + 8s^3 - 3s^4 & \text{if } s \leqslant 1, \\ 0 & \text{if } s > 1 \end{cases} \tag{6}$$

and the normalized distance is

$$s = \frac{\|\mathbf{x} - \mathbf{x}_i\|}{R_i} \tag{7}$$

with R_i the radius of the influence domain of node i. These radii must be large enough to ensure that each point of the domain is covered by at least 3 supports (3 being the size of the basis). According to our experience based on simple test cases with a known exact solution, $R_i = 1.7 \times h$ (where h is the characteristic nodal spacing distance) constitutes a good choice.

The distance s in Eq. (5) must be modified if the line segment joining $\mathbf{x}_i$ and $\mathbf{x}$ crosses a crack line in order to represent the displacement discontinuity across this line. As in [1], s becomes the total length of the shortest path from $\mathbf{x}_i$ to $\mathbf{x}$ that lies entirely within the domain (divided by the radius of the support):

$$s = \frac{\|\mathbf{x} - \mathbf{x}_{\mathrm{c}}\| + \|\mathbf{x}_{\mathrm{c}} - \mathbf{x}_i\|}{R_i}, \tag{8}$$

where $\mathbf{x}_{\mathrm{c}}$ are the coordinates of the crack tip near $\mathbf{x}_i$.

3. Near-tip field enrichment

The meshless method is particularly suitable to simulate crack propagation because no remeshing is necessary. Special care must, however, be taken in order to precisely model the high gradient of the displacement near the crack tip. Otherwise, the SIFs are underestimated and consequently the life of the structure is overestimated. Let us recall that, in the absence of mode III, the near-tip displacement field is given by:

$$\mathbf{u}(\mathbf{x}) = K_{\mathrm{I}}\mathbf{Q}_{\mathrm{I}}(\mathbf{x}) + K_{\mathrm{II}}\mathbf{Q}_{\mathrm{II}}(\mathbf{x}), \tag{9}$$

$$\mathbf{Q}_{\mathrm{I}}(\mathbf{x}) = \tfrac{1}{2\mu}\sqrt{\tfrac{r}{2\pi}} \begin{pmatrix} \cos(\frac{\theta}{2})[\kappa - 1 + 2\sin^2(\frac{\theta}{2})] \\ \sin(\frac{\theta}{2})[\kappa + 1 - 2\cos^2(\frac{\theta}{2})] \end{pmatrix}, \tag{10}$$

$$\mathbf{Q}_{\mathrm{II}}(\mathbf{x}) = \frac{1}{2\mu}\sqrt{\frac{r}{2\pi}}\begin{pmatrix} \sin(\frac{\theta}{2})[\kappa + 1 + 2\cos^2(\frac{\theta}{2})] \\ \cos(\frac{\theta}{2})[-\kappa + 1 + 2\sin^2(\frac{\theta}{2})] \end{pmatrix}, \tag{11}$$

where K_{I} and K_{II} are the modes I and II SIFs, respectively, r is the distance to the tip, θ is the angle measured from a line ahead of the crack ($\theta \in [-\pi, \pi]$), μ is the shear modulus and κ is the Kolosov constant.

Our enriched method consists in adding some nodes with special weight functions at each tip. The guidelines we follow to choose them are the following: the weight functions must possess the behavior in $\sqrt{r}$ for small r; they must have an angular variation of the same kind as those in Eqs. (10) and(11); they must be positive and they must equal zero outside a circular support like the regular weights. We expect the resulting shape functions to be similar to the weight functions as it is the case for the regular nodes and hence, that the displacement field at the tips can be accurately represented. According to some experiments, the use of the three following weights appears to be a good choice:

$$w_{\mathrm{c}}(\mathbf{x}) = \alpha\sqrt{r}\cos\left(\frac{\theta}{2}\right) S_4(s), \tag{12}$$

$$w_{\mathrm{p}}(\mathbf{x}) = \alpha\sqrt{r}\left[1 + \sin\left(\frac{\theta}{2}\right)\right] S_4(s), \tag{13}$$

$$w_{\mathrm{m}}(\mathbf{x}) = \alpha\sqrt{r}\left[1 - \sin\left(\frac{\theta}{2}\right)\right] S_4(s), \tag{14}$$

where c, p and m, respectively, stand for “cos”, “plus sin” and “minus sin”. We note that the three functions $\cos(\theta/2)$, $1 + \sin(\theta/2)$ and $1 - \sin(\theta/2)$ cannot exactly represent the angular variations in Eqs. (10) and(11) but the accuracy of the results in Section 5 will show that this is not necessary. The presence of the quartic spline (6) ensures the local character of the shape functions. The distance s is again given by (7) or (8) and we choose the radius of the influence domain small enough, such that it does not contain any crack kink. The α factor controls the amplitude of the enriched weight compared with the amplitude of the regular nodes; $\alpha = 1$ constitutes a reasonable choice.

Two different enriched meshless methods are presented in [5].

4. Fatigue crack growth analysis

Once the PDEs are solved and the displacement in the solid is known, the SIFs are calculated by conservation integrals converted into a domain form [6]. In mixed-mode problems, auxiliary solutions (10) and (11) are used in two interaction conservation integrals to directly obtain both factors. The integration domain is a square centered on the tip and the half-side of this square is equal to the length of a crack increment; the domain thus does not contain any kink. For constant amplitude cyclic loadings, the range of the SIFs is defined as

$$\Delta K = K_{\max} - K_{\min}, \tag{15}$$

where $K_{\max}$ and $K_{\min}$ are the SIFs corresponding to the maximum ($\sigma_{\max}$) and minimum ($\sigma_{\min}$) applied loads, respectively.

In general, the crack path is a curved path. In our analysis, crack propagation is simulated by successive linear increments. We have to determine the direction and the length of these increments. Several criteria exist for the determination of the direction of crack growth under mixed-mode loading. The most important are: maximum principal stress criterion, maximum energy release rate criterion and minimum strain energy density criterion. These criteria predict kink angles of almost the same size, especially in the case of small or medium mixed-mode ratio K_{II}/K_I. In the present work, the maximum principal stress criterion is used, which postulates that the crack growth occurs in a direction perpendicular to the maximum principal stress. Thus, at each crack tip, the local direction of crack growth θ_c is determined by the condition that the local shear stress is zero, that is (see for example [4] for details):

$$K_I \sin\theta_c + K_{II}(3\cos\theta_c - 1) = 0. \tag{16}$$

Solving this equation gives

$$\theta_c = 2\arctan\left(\frac{K_I - \sqrt{K_I^2 + 8K_{II}^2}}{4K_{II}}\right). \tag{17}$$

According to this criterion, the equivalent mode I SIF is

$$K_{Ieq} = K_I \cos^3\tfrac{\theta_c}{2} - 3K_{II}\cos^2\tfrac{\theta_c}{2}\sin\tfrac{\theta_c}{2}. \tag{18}$$

This equivalent SIF is useful in the unstable fracture criterion below and in the following propagation law. To model the stable crack propagation, we use the generalized Paris' law:

$$\frac{da}{dN} = C(\Delta K_{Ieq})^m, \tag{19}$$

where C and m are material properties, a is the crack length, N is the number of loading cycles and ΔK_{Ieq} is obtained by (18) with ΔK_I and ΔK_{II} instead of K_I and K_{II}. The number of loading cycles required to extend the crack from the initial length to a given length is evaluated by integrating this law with a trapezoidal rule.

A compromise must be made regarding the value of the linear increment length Δa. If the latter is too small, the influence domain of the enriched nodes and the integration domain of the conservation integral are small and this leads to inaccurate results. If it is too long, the piecewise linear path cannot precisely represent the real curved path. For single-cracked bodies, Δa is kept constant. For multi-cracked bodies, we choose a constant value for the maximum increment length Δa_{max}, and after each step we select the principal crack tip as the tip where ΔK_{Ieq} is maximum and then at every crack tip the increment is given by

$$\Delta a = \Delta a_{max}\left(\frac{\Delta K_{Ieq}}{\Delta K_{Ieq,max}}\right)^m, \tag{20}$$

where $\Delta K_{Ieq,max}$ is the range of the equivalent mode I SIF at the principal crack tip and m is the exponent in Paris' law. Accordingly, the increment at the principal crack tip is equal to Δa_{max} and is smaller than this value at other crack tips. We note that the principal tip can change during the propagation.

Instability of the cracked body occurs when $K_{Ieq,max,max} > K_{Ic}$ where K_{Ic} is a material property called the fracture toughness. $K_{Ieq,max,max}$ is the equivalent mode I SIF corresponding to σ_{max} at

the principal crack tip. This condition is the stopping criterion in our method: crack increments are added until this condition is met.

5. Numerical results

5.1. Single centered crack

The first example is a single crack, centered in a square plate under uniform tension. The square side is 2 units and the crack length $2a$ varies from 0.2 to 1.4 units. A set of 21×21 uniformly spaced meshless nodes is used. The fatigue crack growth theory is not applied for this problem; the crack grows by step of 0.1 units at each tip. This is justified because the SIFs are identical at both tips.

In Table 1, we compare the values of $F_I = K_I/\sigma\sqrt{\pi a}$ for this range of a for the classic method, and the new method with the solution in [7]. This table shows the significant improvement of the results when the enriched method is used. For $a = 0.1$, the computed SIF is not as good as for $a \geqslant 0.2$; this is probably due to the overlapping of the supports of the 2 enrichments. The extra cost of the enriched method is weak—only 4% of the CPU cost with respect to the classic method.

5.2. Single centered angled crack

To validate the new method for mixed-mode problems, we consider a static angled crack (18 units long) in a rectangular plate (90×180) under uniform tension ($\sigma = 160$). A set of 19×37 uniformly spaced meshless nodes is used and 4 nodes are added on each side of the crack (Fig. 1).

We plot in Fig. 2 modes I and II SIFs for some values of the crack angle. The new method is better than the classic method for every value of the angle and shows very good agreement with Ref. [7].

5.3. Two internal non-colinear cracks

A rectangular plate (90 mm $\times$ 180 mm) with 2 internal, parallel, non-colinear and non-angled cracks (length $=$10 mm for both) is submitted to a cyclic tension ($\sigma_{max} = 160\,\mathrm{N/mm}$, $\sigma_{min} = 0$) at both ends. The horizontal distance between the two tips close to each other is 15 mm and the vertical

Table 1
Mode I normalized stress intensity factors for the centered crack problem

Half-length of the crack a	0.1	0.2	0.3	0.4	0.5	0.6	0.7
F_I—Ref. [7]	1.014	1.055	1.123	1.216	1.334	1.481	1.68
F_I—Classic method	0.967	1.010	1.075	1.162	1.272	1.408	1.586
Error—Classic method	4.6%	4.3%	4.3%	4.4%	4.6%	4.9%	5.6%
F_I—Enriched method	1.004	1.057	1.125	1.217	1.333	1.477	1.668
Error—Enriched method	0.99%	0.15%	0.14%	0.05%	0.09%	0.26%	0.74%

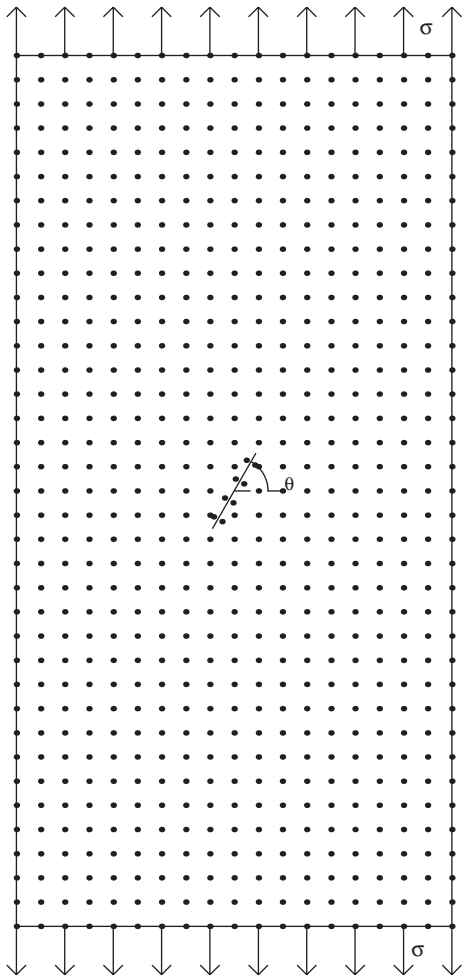

Fig. 1. Set of nodes.

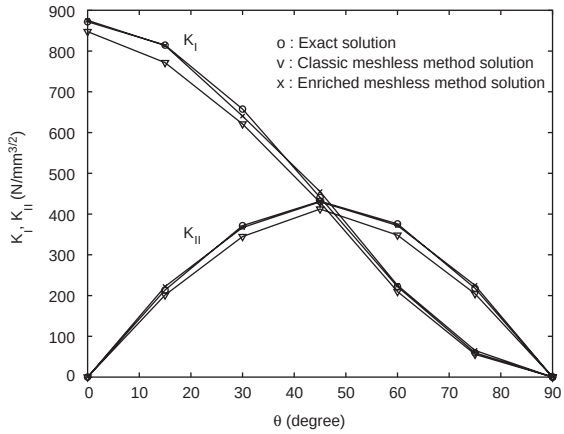

Fig. 2. SIFs for the angled crack.

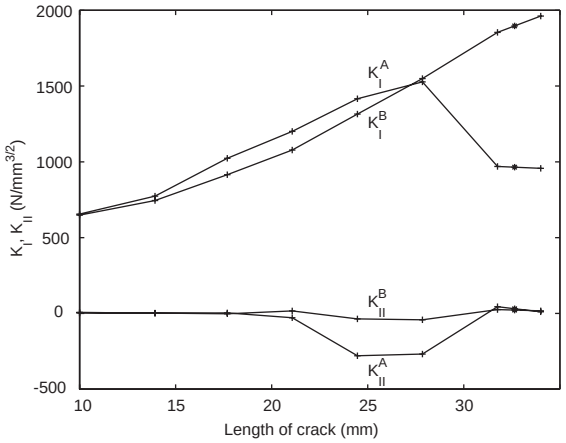

Fig. 3. Stress intensity factors.

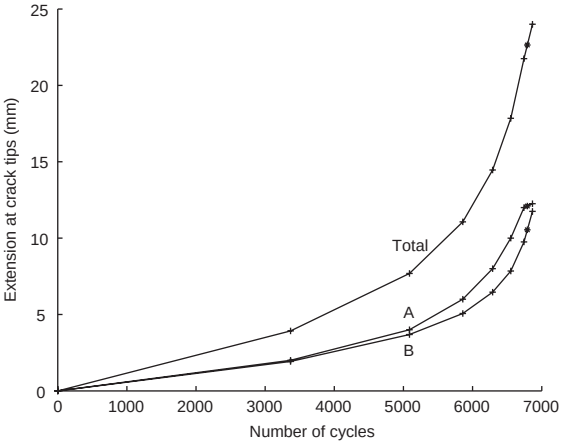

Fig. 4. Fatigue-life diagram.

distance is 5 mm. We use the same dimensions, the same material properties and the same loading as in [9] to perform a comparison: $E = 74000\,\mathrm{N/mm^2}$, $v = 0.3$, $K_{\mathrm{Ic}} = 1897.36\,\mathrm{N/mm^{3/2}}$, $m = 3.32$, $C = 2.087136 \times 10^{-13}$.

We use a regular set of 19×37 meshless nodes plus 2 nodes on each side of both initial cracks and the 3 enriched nodes at each crack tip. When the crack grows, these enriched nodes move with the crack tip and 1 regular node is added on each side of the crack increment. The maximum crack increment length $\Delta a_{\max}$ and the radius of the support of the enriched nodes are equal to 2 mm.

The evolution of the SIFs at the most interior crack tips (A) and at the crack tips near the edge (B) with the crack length is plotted in Fig. 3. The fatigue-life diagram and the crack paths are presented in Figs. 4 and 5, respectively. In the beginning, it is a pure mode I state and the SIFs at A and B are about the same. Then, the mode I factor at A increases more rapidly than at B and

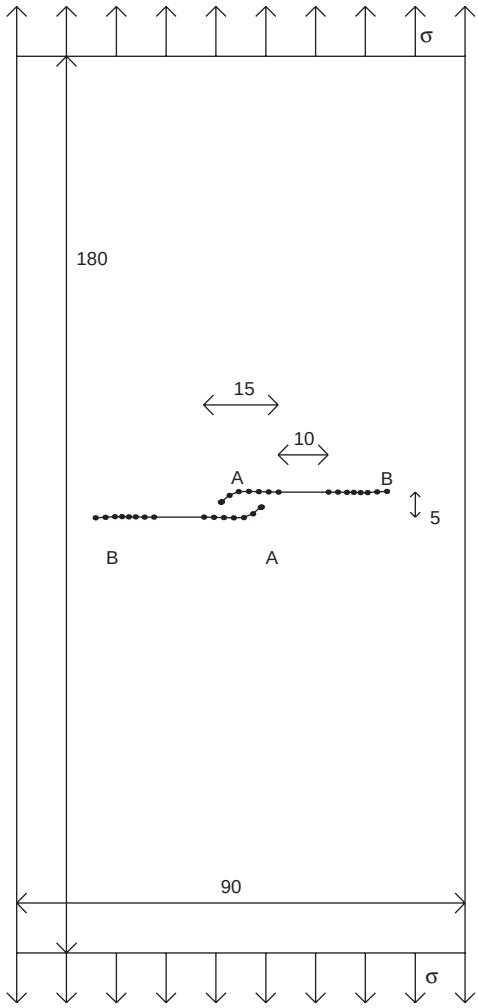

Fig. 5. Crack path for the "two internal cracks" problem.

the mode II factor at A becomes negative so that the crack paths curve towards the other crack. But, when the crack tips A overlap, the SIFs tend to decrease, while the mode I factor continuously increases at B. Finally, the equivalent mode I SIF at B exceeds the fracture toughness and unstable fracture occurs at the crack tips B. This prediction of the fatigue crack growth path is in good agreement with the experimental results reported in [8]. The life of the structure is evaluated as 6792 cycles, which is in good agreement with [9].

Acknowledgements

The support of the Belgian National Fund for Scientific Research (F.N.R.S.) to Marc Duflot is gratefully acknowledged.

References

[1] T. Belytschko, Y. Krongauz, M. Fleming, D. Organ, W.K. Liu, Smoothing and accelerated computations in the element-free Galerkin method, J. Comput. Appl. Math. 74 (1996) 111–126.
[2] T. Belytschko, Y. Krongauz, D. Organ, M. Fleming, P. Krysl, Meshless methods: an overview and recent developments, Comput. Methods Appl. Mech. Eng. 139 (1996) 3–47.
[3] T. Belytschko, Y.Y. Lu, L. Gu, Crack propagation by element-free Galerkin methods, Engrg. Fracture Mech. 51 (1995) 295–315.
[4] D. Broek, Elementary Engineering Fracture Mechanics, Noordhoff International Publishing, Leyden, 1974.
[5] M. Fleming, Y.A. Chu, B. Moran, T. Belytschko, Enriched element-free Galerkin methods for crack tip fields, Internat. J. Numer. Methods Eng. 40 (1997) 1483–1504.
[6] B. Moran, C.F. Shih, Crack tip and associated domain integrals from momentum and energy balance, Engrg. Fracture Mech. 27 (1987) 615–641.
[7] Y. Murakami (Ed.), Stress Intensity Factors Handbook, Pergamon Press, Oxford, 1987.
[8] S.T. Tu, R.Y. Cai, A coupling of boundary elements and singular-integral equations for the solution of fatigue cracked body, in: C.A. Brebbia (Ed.), Boundary Elements X, Vol. 3, Computational Mechanics Publisher, 1988, pp. 239–247.
[9] A.M. Yan, H. Nguyen-Dang, Multiple-cracked fatigue crack growth by BEM, Comput. Mech. 16 (1995) 273–280.